Relation between magnetic field and convective cells morphology

Jose Iván Campos Rozo[1], Jan Jurčak[1], Michiel Van Noort[2]

1. Astronomical Institute of the Czech Academy of Sciences, Fricova 298, 25165 Ondrejov, Czech Republic
2. Max-Planck Institute for Solar System Research, Justus-von-Liebig-Weg 3, 37077 Göttingen, Germany

Introduction

Solar granulation typically measures ~1" in quiet Sun regions (e.g., Wohl & Nordlund 1985; Danilovic et al. 2008), with smaller cells below 600 km (Abramenko et al. 2012). **The presence of magnetic field significantly influence granulation properties at both large and small scales, such as sunspots** (Schussler & Vogler 2006; Tiwari et al. 2013) **and flux emergence regions** (Centeno et al. 2016). To study these dynamics, techniques like local correlation tracking (LCT; November & Simon 1988) have been widely applied to measure horizontal apparent motion, meanwhile induction local correlation tracking (ILCT; Welsch et al. 2004) and differential affine velocity estimator (DAVE; Schuck 2006) are applied to track magnetic elements motions. **Characterizing solar structures objectively requires advanced segmentation algorithms**. More sophisticated techniques, such as the multi-threshold algorithm MLT4 (Bovelet and Wiehr 2007), have been developed to address these challenges and accurately identify photospheric structure

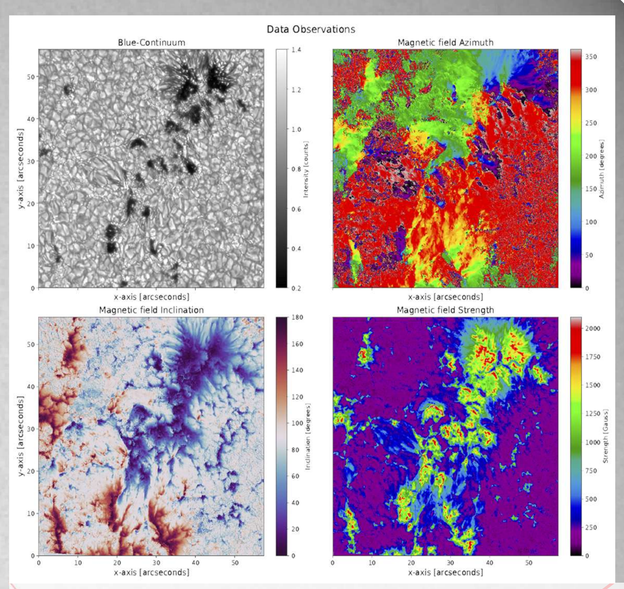

Figure 1: Co-aligned blue-continuum and CRISP vector magnetic field data. The observed data is rotated ~55° with respect to the up north direction of the Sun (reference HMI/SDO image). Top-left: clipped blue-continuum image. Top-right: magnetic field azimuth angle in the range 0°-360°. Bottom-left: magnetic field inclination angle in the range 0°-180°. Bottom-right: magnetic field strength. Vector magnetic field is disambiguated, and transformed to the local reference frame.

Data

On June 13, 2013, the Swedish Solar Telescope (Scharmer et al. 2003) observed the evolving active region NOAA 11768. The study used two datasets:

1. **Blue continuum images reconstructed with MOMFBD (van Noort et al. 2005), recorded from 8:21-10:50 UT, with 5.6-second cadence and 0.034" spatial sampling.**
2. **CRISP observations (Scharmer et al. 2008) of Fe I 525 nm lines recored the stokes profiles from 8:36-10:54 UT, with ~31 second cadence and 0.058" spatial sampling.**

The datasets were co-aligned and resampled to matching spatial resolutions. Granule segmentation was performed using the MLT4 algorithm. Magnetic field vector was derived from CRISP data using VFISV (Borrero et al. 2011), with 180° ambiguity resolved by using AMBIG (Leka et al. 2009) and local reference frame transformation. Sample data is showed in Figure 1.

Analysis and Results

Figure 2 displays the segmented mask obtained from a 5-minutes average intensity image with the strong magnetic field areas also removed, and applied to the vector magnetic field images.The observed field of view (FOV) shows a large variety array of granulation phenomena, including:

1. **Convection in non-magnetized regions (upper-left and lower-right areas of the FOV)**
2. **Granulation around pores magnetized regions.**
3. **Magnetic field emergence regions.**

We applied the segmented mask to the diverent observed parameters, and we obtain information about:

1. **From the intensity images: area, eccentricity, and mean intensity per segment.**
2. **From the magnetic field vector: magnetic field intensity, inclination and azimuth.**
3. **From proper motions calculations: magnitude of the aparent motions, and divergences of the horizontal flow fields.**

Current analysis does not include temporal evolution of granules.

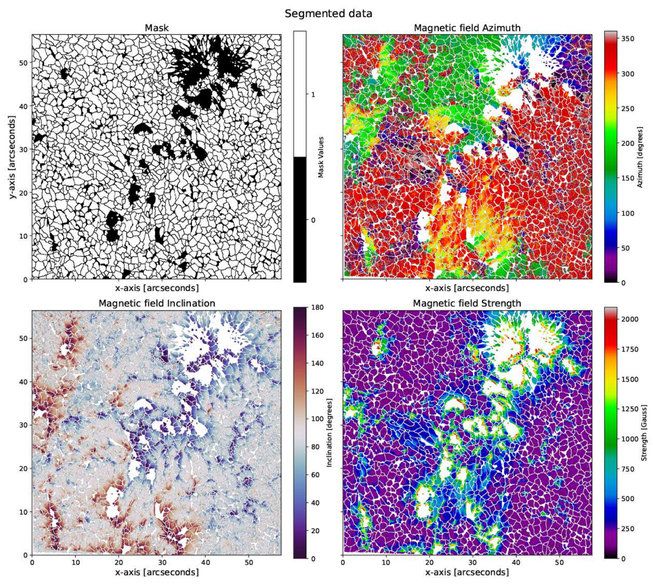

Figure 2: From left to right: Mask obtained from the segmentation algorithm. The mask was applied to an average intensity image, to the vector magnetic field images (as the figures shows), and the the apparent motions obtained with different algorithms.

Figure 3 presents dispersion plots over kernel distribution estimation (KDE) maps illustrating relationships between magnetic fields and convective cell properties in solar granulation. Panel (a) shows a correlation between granule size and magnetic field strength, with the largest granules in non-magnetized regions with the strongest fields are predominantly vertical. Panel (b) displays how the vertical magnetic field component (B_{ver}) increases meanwhile mean granule intensity decreases. Panels (c), and (e) explore relationships between apparent motion divergence, granule size, mean segment intensity, continuum intensity, and proper motion magnitude in relation to magnetic field strength. These analyses provide insights into plasma flow dynamics and the suppression of convective motions in magnetized regions. Panel (d) shows thst in regions where the strength of the magnetic field increases, the intensity of the granulation decreases.

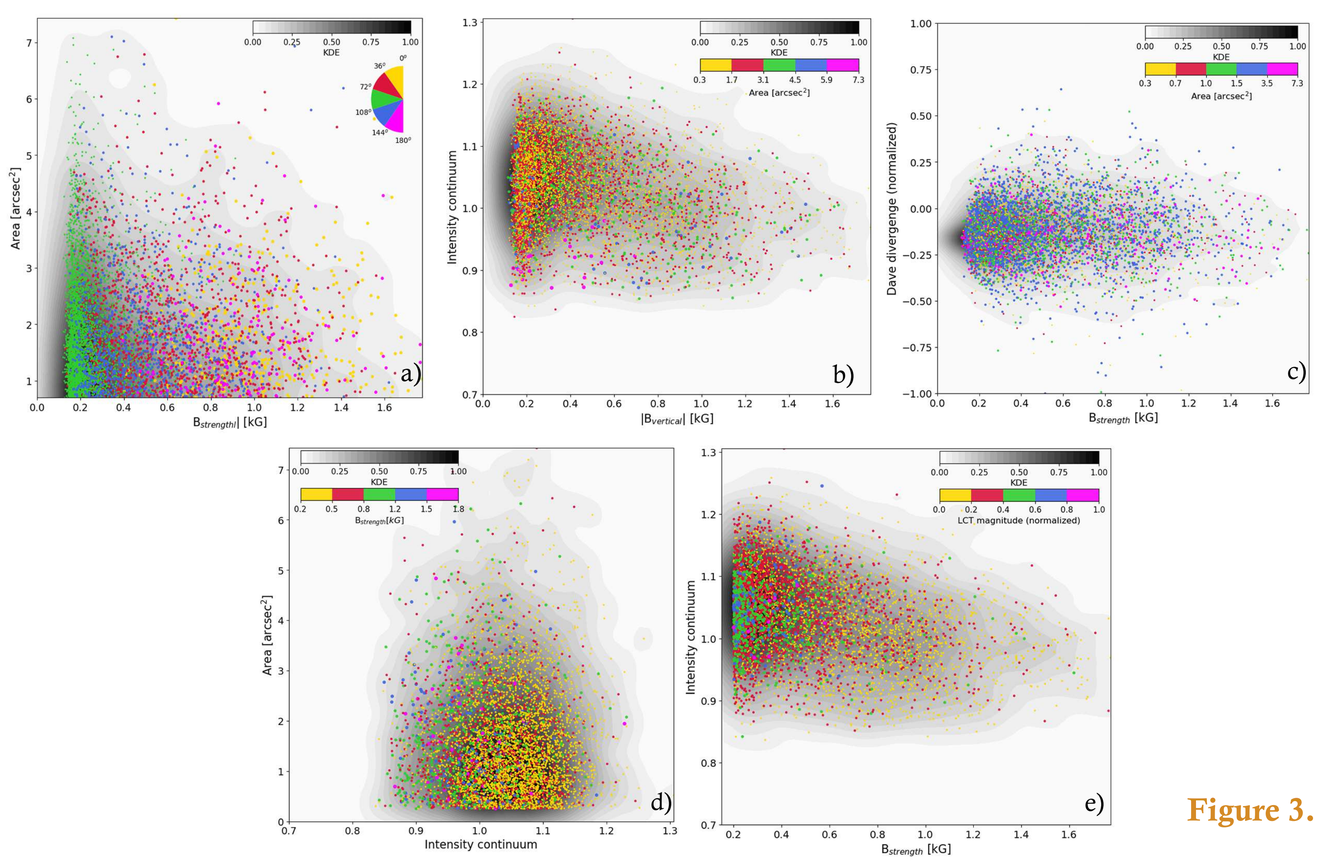

Figure 3.

Discussion and Conclusions

We performed a **statistical analysis of convective cell properties in magnetized and no-magnetized regions** using SST observations. Our FOV covered a large amount of diverse granulation phenomena, from quiet Sun convection to sunspot magneto-convection. The findings, illustrated in Figure 3, corroborate and extend previous studies on magnetized convection. We observed an performed correlations between granule morphology features and magnetic field prooperties, finding a strong relationship between a decrease in granule intensity with the increasing of vertical magnetic field. **Mean divergence of the apparent magnetic elements velocity in granules decreased with increasing magnetic field strength.** For future work, we propose implementing a tracking algorithm for segmented granules obtained in this work, studying convective cell lifetime dependence on magnetic field presence and refining our analysis by considering temporal evolution of magnetic properties and apparent motions This approach will provide deeper insights into solar surface convection dynamics across various magnetic environment

References

[1] Woehl, H., & Nordlund, A. 1985 Solar Phys., 97, 213.
[2] Danilovic, S., Gandorfer, A., Lagg, A., Sch¨ussler, M., Solanki, S. K., V¨ogler, A., Katsukawa, Y., & Tsuneta, S. 2008, A&A, 484, 17
[3] November,L. J. and Simon,G.W.: 1988, Astrophys. J.333, 427.
[4] Abramenko, V. I., Yurchyshyn, V. B., Goode, P. R., Kitiashvili, I. N., & Kosovichev, A. G. 2012, ApJ, 756, L27
[5] Schüssler, M., & Vögler, A. 2006 ApJ, 641, 73
[6] Tiwari, S. K., van Noort, M., Lagg, A., & Solanki, S. K. 2013 A&A, 557, 25
[7] Centeno, R., et al. 2016, arXiv, 2016arXiv161003531C
[8] Welsch, B. T., Fisher, G. H., Abbett, W. P., & Regnier, S. 2004, ApJ,610, 1148
[9] Schuck, P. W. 2006, ApJ, 646, 1358
[10] Bovelet, B., & Wiehr, E. 2007, Sol. Phys., 243, 121.
[11] Scharmer, G. B., et al. 2003 SPIE, 4853, 341
[12] Scharmer, G. B., et al. 2008 ApJ, 689, 69.
[13] van Noort, M., et al. 2005 Solar Phys., 228, 191
[14] Leka, K. D., Barnes, G., & Crouch, A. 2009 ASPC, 415, 365.
[15] Borrero, J. M., et al. 2011, Solar Phys., 273, 267

Aknowledgments

This work was supported by the Czech-German common grant, funded by he Czech Science Foundation under the project 23-07633K and by the Deutsche Forschungsgemeinschaft under the project BE 5771/3-1 (eBer-23-13412).